SAND2008-0469C

Power scaling of fiber-based amplifiers seeded with microchip lasers

Paul E. Schrader[a], Jean-Philippe Fève*[b], Roger L. Farrow[a], Dahv A.V. Kliner[a], Randal L. Schmitt[c], and Binh T. Do[c]
[a]Sandia National Laboratories P.O. Box 969, MS 9056, Livermore, CA 94551
[b]JDSU, Commercial Lasers Group, 430 N. McCarthy Blvd., Milpitas CA 95035
[c]Sandia National Laboratories, P.O. Box 5800, Albuquerque, NM 87185
*jean-philippe.feve@jdsu.com

ABSTRACT

We summarize the performance of mode-filtered, Yb-doped fiber amplifiers seeded by microchip lasers with nanosecond-duration pulses. These systems offer the advantages of compactness, efficiency, high peak power, diffraction-limited beam quality, and widely variable pulse energy and repetition rate. We review the fundamental limits on pulsed fiber amplifiers imposed by nonlinear processes, with a focus on the specific regime of nanosecond pulses. Different design options for the fiber and the seed laser are discussed, including the effects of pulse duration, wavelength, and linewidth. We show an example of a microchip-seeded, single-stage, single-pass fiber amplifier that produced pulses with 1.1 MW peak power, 0.76 mJ pulse energy, smooth temporal and spectral profiles, diffraction-limited beam quality, and linear polarization.

Keywords: fiber amplifier, fiber laser, double-clad fiber, mode filtering, microlaser, nonlinear optics, four-wave mixing

1. INTRODUCTION

Pulsed fiber amplifiers are very attractive laser sources for materials processing, printing, lidar, and nonlinear frequency conversion because of their ability to deliver pulses with very high average and peak powers and diffraction-limited beam quality in highly reliable devices. Recent developments in double-clad, Yb-doped, large-mode-area (LMA) fibers have led to a record combination of average and peak output powers at 1064 nm.[1-3] Due to the very high peak irradiances of the amplified pulses, nonlinear effects remain the limiting factor for power scaling. Different techniques have successfully been implemented to increase the effective mode field area and so increase the threshold power for the nonlinear effects while preserving single-mode output in large-core fibers.[4-8] The relative importance of the different nonlinear processes depends on the pulse temporal and spectral characteristics; in Section 2, we discuss these limitations and emphasize the specific advantages of microchip lasers as seeds. In 1.0 ns, 1064 nm, pulsed fiber amplifiers, we have shown previously that four-wave-mixing (FWM) sets the limit to the pulse energy,[9,10] and in Section 2 we review its importance relative to stimulated Raman scattering (SRS). In Section 3, we examine tradeoffs for design optimization of pulsed fiber amplifiers. Finally, we show experimental results for a system based on a LMA fiber with 50 μm core diameter and a microchip seed laser at 1030 nm, which generated pulses with high energy (0.76 mJ), high peak power (1.1 MW), smooth temporal and spectral profiles, and linear output polarization; given its diffraction-limited beam quality and linear polarization, this system is an ideal pump source for nonlinear optical frequency conversion, as demonstrated recently.[11]

2. GENERAL CONSIDERATIONS ON NONLINEAR EFFECTS

2.1 Nonlinear processes

Depending on the pulse duration and spectral linewidth of the amplified beam, the relative importance of the different nonlinear effects changes significantly, as has been discussed widely in the past.[12] In this section, we review their respective contributions, which allows us to point out the specific advantages of passively Q-switched microchip lasers as seed sources and to derive a few important rules for the design of fiber-based high-power amplifiers.

Figure 1 shows the characteristic average powers and pulse energies corresponding to the onset of self-phase modulation (SPM), SRS, stimulated Brillouin scattering (SBS), FWM, self-focusing (SF), and optical damage. This calculation

considers a repetition rate of 100 kHz, which is of interest for many applications, but scaling of the right-hand axis (pulse energy) provides the corresponding average power for other repetition rates. The calculation assumes a 3 m long LMA fiber with an effective area of 511 μm^2, typical of a 30 μm core-diameter fiber with a numerical aperture (NA) of 0.06. LMA fibers and photonic crystal fibers with core diameters larger than 50 μm have been reported; because the threshold powers of all nonlinear effects except SF scale with the effective area, all of the curves except SF will shift vertically for such fibers, but their relative position will not change. However, the core diameter and NA of the fiber have practical limitations: manufacturability, bend sensitivity, difficulty of cleaving and splicing, and stability and reproducibility of the beam profile must be considered for the design of an actual system, and Fig. 1 represents a realistic trade-off for current fibers. For such fibers, SF and optical damage are not a concern because the peak irradiance is always limited to lower values by nonlinear effects; this conclusion would not hold for larger fibers with correspondingly higher maximum peak powers or for fibers that do not achieve the damage thresholds observed for high-quality fibers. For long pulse durations (greater than ~2 ns) with transform-limited linewidths, stimulated Brillouin scattering (SBS) is the most limiting nonlinear process. Specially designed fibers have been developed for mitigating SBS by reducing the overlap of the acoustic wave with the core.[13,14] As the pulse duration is shortened, the threshold power for SBS increases steeply because (1) the linewidth of a transform-limited pulse exceeds the Brillouin gain bandwidth (typically ~50-100 MHz), (2) SPM further increases the linewidth (especially for sub-ns pulses), and (3) the spatial overlap of the amplified pulse and the counter-propagating SBS pulse becomes shorter than the length of the fiber amplifier. These factors prevent SBS for pulse durations below ~1 ns (the exact value depends on the details of the fiber and seed source). Further decreasing the pulse duration is detrimental for maximizing the pulse energy or minimizing the linewidth (e.g., for efficient nonlinear frequency conversion).

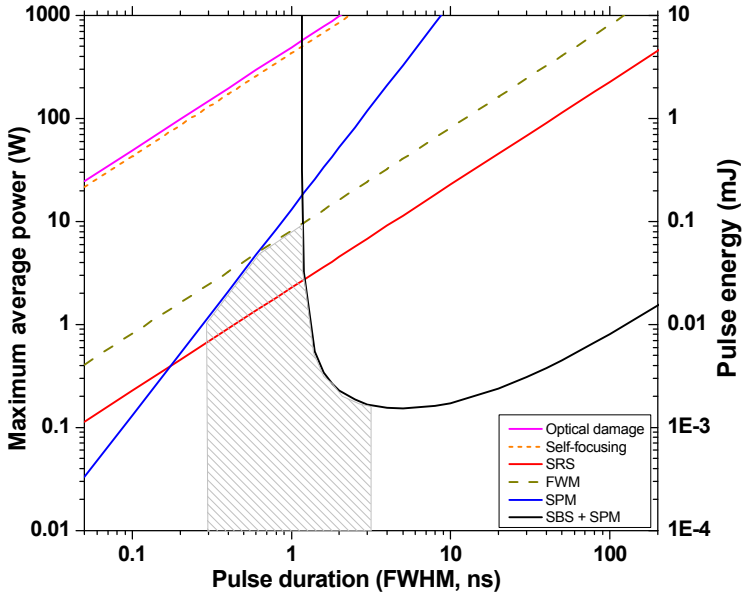

Fig. 1. Calculated average power limitations induced by the different nonlinear effects, for a repetition rate f = 100 kHz, in a 3 m long LMA fiber with an effective mode area of 511 μm^2. The threshold power for SRS is deduced from Ref. 12. The critical power for SF is deduced from Ref. 16. The optical damage irradiance is taken from Ref. 17. The maximum power for FWM is from Ref. 10, with Δk = 50 m^{-1}. For SPM, the limit corresponds to a spectral broadening less than 0.25 nm. For SBS, we calculated the threshold power by multiplying the cw value by the ratio of the Brillouin gain bandwidth to the laser linewidth, taking into account spectral broadening due to SPM.

The curves in Fig. 1 are meant as guidelines, showing the relative importance of various nonlinear processes; quantitative details will depend on specific characteristics of the seed source (wavelength, temporal pulse shape, spectrum, etc.) and the fiber amplifier (length, doping level, pump wavelength, etc.). Nonetheless, this analysis provides very useful guidance for optimizing fiber-amplifier performance. The shaded area in Fig. 1 shows that a pulse duration of ~1 ns is highly suitable for maximizing the output power in high-energy pulsed fiber amplifiers with minimum spectral and temporal distortion, as confirmed in several experiments.[2,15] In this regime, SRS generally becomes the most limiting effect.[1,4,12] The red curve in Fig. 1 is not a hard limit but represents a threshold power above which an increasing fraction of the pulse energy will appear in the Stokes band. FWM would not be phase-matched in a passive fiber, but as

shown theoretically and experimentally,[9,10] the presence of gain allows efficient FWM, which sets an upper limit to the in-band pulse energy, beyond which all photons are converted to out-of-band wavelengths. This process also strongly impacts the spectrum and temporal profile of the output pulses, so that FWM is the actual limiting effect in 1 ns pulsed fiber amplifiers.

In order to provide a better understanding of the relative importance of SRS and FWM in a fiber amplifier seeded with 1-ns pulses, Fig. 2 shows calculations of the amplified field at 1064 nm (the seed wavelength) and 1084 nm (a FWM signal wavelength) in a LMA fiber amplifier using the fiber parameters of Ref. 9. We also consider the same fiber amplifier, with similar seed pulses and pumping conditions, but with either no SRS or no FWM.

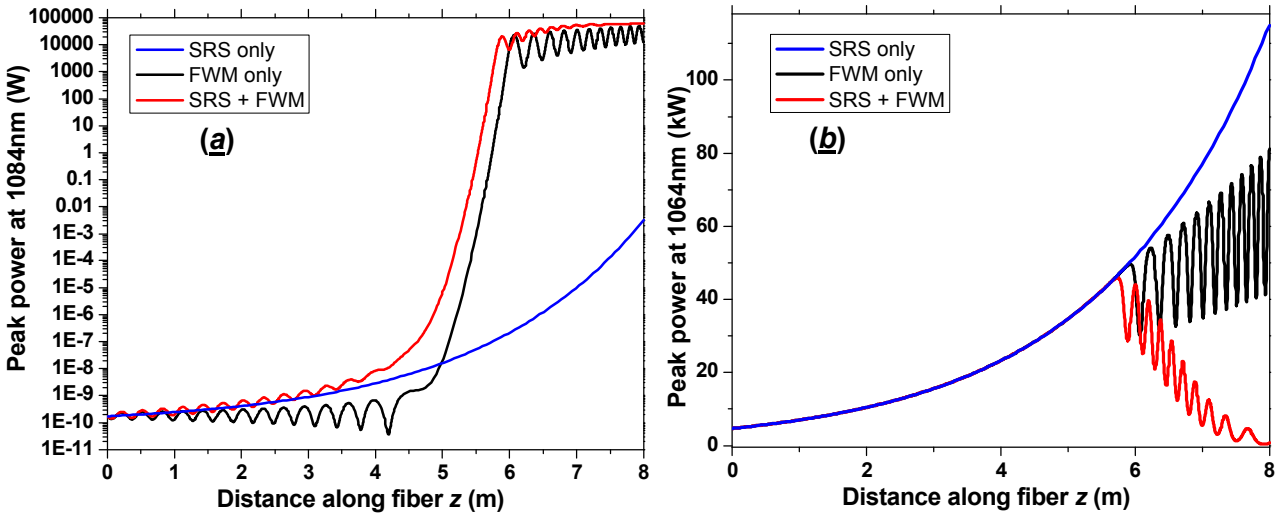

Fig. 2. Peak powers along the fiber: (a) wave generated by FWM ("signal" λ_3 = 1084 nm); (b) amplified wave ("pump", λ_1 = 1064 nm). The 8 m long LMA fiber has an effective area of 511 μm^2 and the gain is g = 0.4 m^{-1}; the seed pulses have a duration of 1 ns FWHM and energy of 5 μJ. The nonlinear and Raman coefficients for the different curves are: blue (n_2 = 0 m²/W, g_R = 1.2x10^{-13} m²/W); black (n_2 = 2.7x10^{-20} m²/W, g_R = 0 m²/W); red (n_2 = 2.7x10^{-20} m²/W, g_R = 1.2x10^{-13} m²/W).

The simulations in Fig. 2a show that the 1084 nm fields generated by these two nonlinear processes exhibit very different behavior. Whereas SRS is not very efficient because the signal wavelength is not matched to the peak of the Raman gain, FWM can generate a very high power even though the phase-mismatch is relatively large; because of "gain-induced phase-matching", the sinusoidal variation of the signal field at the entrance of the fiber gradually turns into an exponential-like variation as the peak power is increased, as expected from the asymptotic expressions in Ref. 9. Figure 2b shows the corresponding amplified field at 1064 nm. Whereas SRS is too weak to cause a significant impact, FWM alone can induce large depletion and limit the output power. However, complete depletion of the beam at 1064 nm is only reached through further amplification of the 1084 nm field by Raman gain.

In an active fiber, the presence of gain allows efficient FWM, which in turns acts as a seed for SRS and greatly exacerbates its effect. Re-examining Fig. 1 with this picture in mind, the maximum power corresponding to SRS should not be seen as a hard limit, since this is a threshold power. In contrast, the upper limit set by FWM is a real maximum for a given fiber, beyond which full depletion leads only to generation of out-of-band wavelengths. The shaded area representing the power that can be generated by the amplifier is then ultimately limited by FWM combined with SRS. Figure 1 also shows that the design window for the pulse duration of such a high-power amplifier is narrow: ~0.7 ns to ~1.4 ns; beyond these limits, the pulse energy and corresponding peak power are restricted to lower values by SPM (for shorter pulses) and SBS (for longer pulses).

2.2 Microchip-laser seed sources

Most microchip lasers employ a Nd^{3+}-doped crystalline gain medium and a Cr^{4+}:YAG saturable absorber as the Q-switch (alternative designs are discussed below). These passively Q-switched lasers offer numerous advantages as seed sources for high-power pulsed fiber amplifiers:

- Given their cavity length, the pulse duration typically falls in the ns range.

- Different materials for the saturable absorber and/or the gain medium provide access to a wide range of pulse energies and repetition rates and to different wavelengths.[15,18,19]
- They do no require high-voltage or high-speed driving electronics.
- They allow robust and compact packaging.
- Their diffraction-limited beam quality is ideal for efficiently seeding mode-filtered and other LMA fiber amplifiers.
- Because of their high peak power, no pre-amplification stages (and their associated isolation optics) are required.
- Because they do not generate a significant cw background or out-of-band wavelengths (amplified spontaneous emission, ASE), no spectral filtering or time-gating is required for seeding the amplifier. This point is illustrated in Fig. 3, which shows the spectrum of an LMA fiber amplifier seeded with an actively Q-switched fiber laser that generates ASE.[20] SRS and FWM generate out-of-band wavelengths in the fiber. Although these effects are weak in the oscillator (-30 dB at maximum), the out-of-band fraction is much higher at the output of the amplifier because ASE from the seed source partially saturates the gain in the amplifier. Using a narrow bandpass filter at the output of the oscillator strongly reduces but does not eliminate the out-of-band power. In comparison, a microchip seed laser leads to a simpler architecture, with no need to control the seed spectral or temporal characteristics.

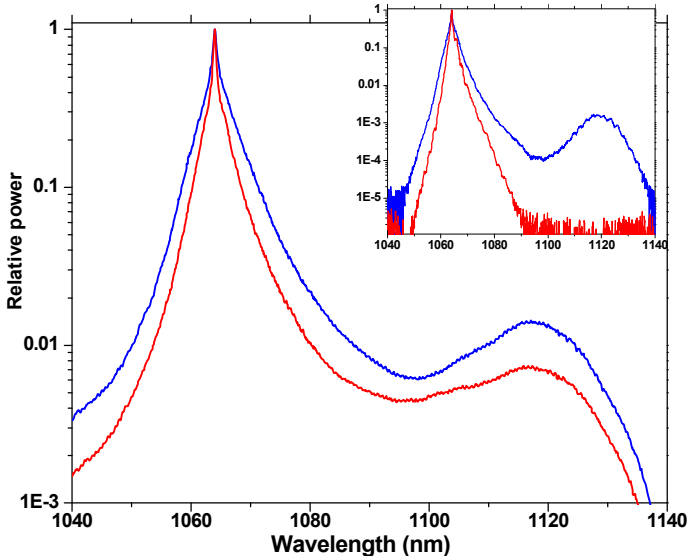

Fig. 3. Output spectra of a 4 m long LMA fiber amplifier seeded by an actively Q-switched fiber laser (Ref. 20); repetition rate 20 kHz, pulse duration 55 ns, output power 10 W. The inset shows the corresponding spectra of the seed laser. Blue curves are for an unfiltered seed beam, whereas a 10 nm FWHM bandpass filter was added for the red curves.

For development of a product capable of volume industrial production, the design must accommodate variations in performance within and among batches of microlasers, mainly arising from variations in the reflectivity of the output coupler and in the saturable losses of the Q-switch. Given the narrow design window for the pulse duration (Section 2.1), the target pulse duration should thus be set as close as possible to 1 ns, which in turn limits the accessible range of repetition rate and pulse energy.[11]

3. OPTIMIZATION

In this section, we review general design rules for high-power pulsed fiber amplifiers with the goal of minimizing the temporal and spectral distortions due to nonlinear effects and preserving diffraction-limited beam quality and linear polarization. We also examine the tradeoffs involved in the design of an industrial system compatible with volume manufacturing, which imposes more significant constraints than those associated with laboratory systems.

3.1 Fiber design

Because the threshold power of all nonlinear effects except SF is inversely proportional to the fiber length, the usual optimization rule is to increase the core-to-cladding area ratio and to maximize the Yb concentration, both of which allow the fiber length to be minimized by increasing the pump absorption coefficient. The intrinsic brightness (radiance) of the pump source, loss of brightness by the pump-coupling method (Section 3.2), and the attainable NA of the inner cladding set the lower limit on the cladding diameter. The upper limit on the core diameter is determined by fabrication issues and the ability to maintain a diffraction-limited output beam (see below); increasing this limit is an active area of research. The maximum Yb concentration is determined by the solubility of Yb in the host glass and by the fiber-fabrication method; higher doping levels have been associated with increased photodarkening in some fibers, although other aspects of fiber composition and fabrication influence photodarkening.[21] The initial rate of photodarkening has been shown to depend strongly on the concentration of excited-state Yb^{3+} ions, and a given fiber will thus photodarken more rapidly at high inversion levels, such as those typically found in pulsed amplifiers.[21] Current research efforts are directed at developing a mechanistic understanding of and mitigating photodarkening.[22]

The threshold power of all nonlinear effects except SF increases with the effective area of the fiber, and many approaches have been proposed to increase the mode field diameter while maintaining diffraction-limited beam quality.[4-8,23] When designing a laser system for volume production, one needs to take into account the reproducibility and the stability of the optical performance parameters, which set practical limits on the core diameter and NA (and hence mode field area) and on the Yb doping level. Key issues include bend sensitivity of the fiber (for packaging and handling), maintaining diffraction-limited beam quality, difficulty of cleaving and splicing the fiber, availability of pump combiners with matched dimensions (Section 3.2), and susceptibility to photodarkening. Active research and development efforts focused on novel fiber designs and improved process control during fiber fabrication have resulted in significant advances in all of these areas. Although the technology employed in a commercial laser system typically represents a compromise among the above considerations, further developments are expected to allow the performance of commercial systems to approach that of the laboratory systems described below and in Refs. 2, 3, 11, and 15.

3.2 Pumping method

In addition to preservation of pump power and brightness, numerous considerations place stringent demands on the pump-coupling technology. Counter-propagating the pump and seed beams reduces the propagation length of the high-peak-power amplified field in the fiber (i.e., reduces the effective interaction length for nonlinear processes) and is thus preferred for reducing nonlinear effects. Transmission of the amplified signal must be maximized while preserving the output beam quality and polarization state. For long-term reliability and for high-power operation, glass-clad fiber is preferred over fiber employing a low-index polymer outer cladding, and the pumping method should be compatible with such fiber; passive glass-clad fibers are commercially available and are routinely deployed in harsh environments, but glass-clad rare-earth-doped fibers are not yet widely available and tested. A common failure mechanism is partial coupling of the high-peak-power amplified pulses into the pump diodes; the pump coupler thus needs to provide high isolation between the pump and signal channels.

In the case of a fiber-based coupler, additional fiber length should be minimized to avoid inducing nonlinear effects, and easy, low-loss splicing to the active fiber is required. Although the possibility of all-fiber architectures has been promoted as a compelling advantage of fiber sources, because of the above considerations, most published results have employed free-space pump-coupling techniques, especially at record peak powers and pulse energies.[1-3,11,15] Existing fused-fiber pump couplers do not meet all of the above requirements, and they are not available for the full range of LMA fibers produced commercially. Current industrial pulsed fiber amplifiers based on fused-fiber combiners primarily use a co-propagating architecture with filters for isolation of the diodes against backward-propagating signal light; the attainable performance is thus compromised to achieve higher reliability and ruggedness.

Pumping at the peak absorption wavelength (976 nm for Yb-doped fibers) is desired, but the output spectrum of most pump diodes is broad relative to the sharp 976-nm absorption peak (9 nm FWHM for the absorption cross section), which reduces the effective pump absorption coefficient, and the diode spectrum is temperature sensitive (typically 0.3 nm/°C). Wavelength-stabilized pump diodes are now commercially available. These sources have a narrow output spectrum (<1 nm FWHM) and a lower temperature sensitivity (<0.07 nm/°C), thereby providing much higher and more stable pump absorption; furthermore, eliminating the need to carefully temperature regulate the pump diode can substantially reduce system power consumption. Continued development of wavelength-stabilized pump sources will make them the preferred choice for high-power fiber sources (pulsed and cw).

3.3 Effect of seed wavelength

Passively Q-switched microlasers used for seeding pulsed fiber amplifiers have been based primarily on Nd^{3+} as the lasing element. Although different host matrices have been tested, such as YAG, LSB and $GdVO_4$,[11,15,18] the lasing wavelength has remained in the narrow range of 1062-1064 nm. The gain spectrum of a Yb-doped fiber amplifier depends on the fiber length because of the quasi-three-level nature of the transition; short amplifiers, which are preferred for minimizing nonlinear processes (Section 3.1), have maximum gain near 1030 nm, significantly bluer than the ~1060 nm emission of Nd-based microchip lasers. Microlasers with a shorter lasing wavelength are thus a compelling solution for increasing the efficiency and pulse energy of fiber amplifiers.

We recently developed a family of passively Q-switched microlasers using Yb^{3+}:YAG as the gain medium whose output wavelength of 1030.6 nm is well matched to the peak gain of Yb-doped fiber amplifiers. These lasers provide pulse durations of 0.5-1.0 ns at repetition rates of up to 19 kHz.[19] In general, Yb^{3+}:YAG microlasers can produce higher pulse energies (because of a lower stimulated emission cross section) and operate with higher optical-to-optical efficiency (because of a lower quantum defect) than similar Nd^{3+}-based microlasers. Figure 4 compares the output power of a fiber amplifier seeded at 1030.6 nm using a Yb^{3+}:YAG microlaser and at 1062.4 nm using a commercial Nd^{3+}:LSB microlaser (Standa); these seed lasers have the same pulse duration, repetition rate, and pulse energy. The LMA fiber (Liekki) had a 27.9 μm core diameter, 0.07 core NA, 250 μm inner-cladding diameter, and 1.5 m length;, a high Yb concentration provided high pump absorption (11.2 dB/m at 976 nm). The fiber was coiled on orthogonal spools with a radius of 5.4 cm for mode filtering.[4] According to the cross sections at the two seed wavelengths listed in Table 1, the power required for reaching transparency is higher at 1030.6 nm. As a consequence, as can be seen in the inset of Fig. 4, at low pump power the output energy was higher at the longer wavelength. However, when the pump power was high enough to provide efficient amplification, the shorter wavelength led to higher output energy. In Fig. 4, the maximum pulse energy at 1030.6 nm is 40% higher than that at 1062.4 nm, which is a significant improvement in the efficiency of the amplifier.

Table 1. Absorption and emission cross sections of Yb^{3+} (σ_{ab} and σ_{em} respectively) for the two seed wavelengths (λ_s) taken from Liekki Application Designer software. The corresponding transparency inversion (P_{tr}) is the population inversion required to reach transparency at λ_s, which is directly proportional to the pump power needed to achieve transparency.

λ_s (nm)	σ_{ab} (10^{-25} m^2)	σ_{em} (10^{-25} m^2)	$P_{tr} = \sigma_{ab} / (\sigma_{ab} + \sigma_{em})$
1030.6	0.437	6.37	6.4 %
1062.4	0.0374	2.55	1.4 %

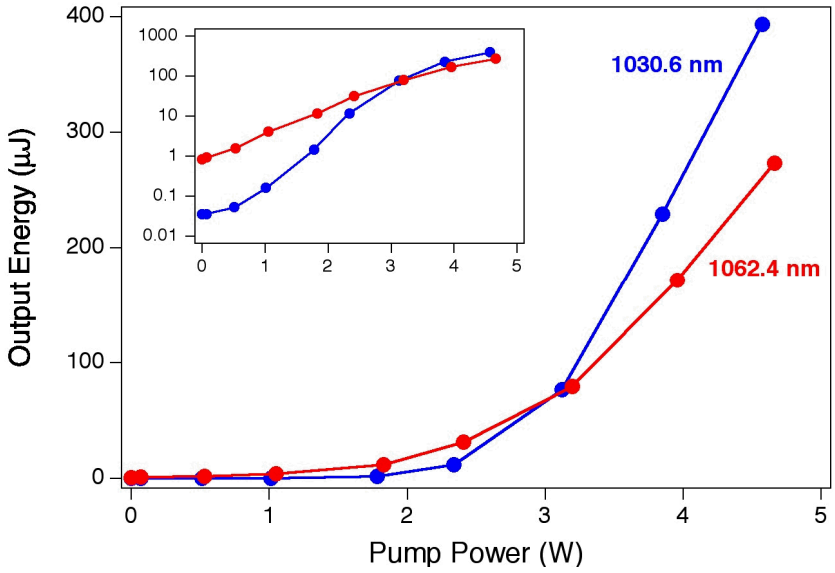

Fig. 4. Output energy of a 1.5 m long LMA fiber amplifier as a function of the pump power for two different seed wavelengths. Both seed microlasers had a repetition rate of 1 kHz, pulse duration of 0.6 ns FWHM, and pulse energy of 4 μJ. Insert is a semi-log version for better comparison at low pump powers.

3.4 Effect of after-pulsing

Most passively Q-switched microlasers exhibit so-called after-pulsing: a secondary pulse with lower energy is emitted several nanoseconds after the main pulse. This phenomenon is due to lasing of a second longitudinal mode in the microchip, and it is commonly observed when the cavity supports more than one longitudinal mode within the gain curve (which pertains to Nd^{3+}:YAG microchip lasers with the target pulse duration of 1 ns). The after-pulse is undesirable for several reasons: it is a source of timing jitter; it can reduce the available gain in high-repetition-rate fiber amplifiers; it typically has a longer duration and thus narrower linewidth than the primary pulse and can therefore generate SBS in the fiber; and it can complicate measurements in lidar and ranging applications.

An alternative would be to use a semiconductor saturable absorber mirror rather than the Cr^{4+}:YAG saturable absorber, but the pulse energy would be too low for efficiently extracting the stored energy from the fiber amplifier.[24] We were able to operate our Yb^{3+}:YAG microlaser (Section 3.3) on a single longitudinal mode (with no after-pulse) up to a repetition rate of 19 kHz.[19] Shot-to-shot mode-hopping was observed at higher repetition rates. The absence of an after-pulse is a distinct advantage of these Yb^{3+}:YAG microlasers. However, the extremely wide gain bandwidth of Yb^{3+}:YAG (~10 times that of Nd^{3+}:YAG) makes single-mode operation challenging at high repetition rates, and the quasi-three-level nature of the lasing transition makes thermal effects more problematic. As with Nd^{3+}-based microlasers, there is a trade-off between the maximum repetition rate, output pulse energy and pulse duration. With Nd^{3+}:YAG microlasers operating in the nanosecond regime, careful design of the microchip, adjustment of the pump parameters, and proper thermal management of the microlaser have allowed operation over a wide range of repetition rates while controlling the timing and amplitude of the secondary pulse.[11,25]

Figure 5a shows the energy in the secondary pulse relative to the primary pulse at the output of the amplifier as a function of pump power. For a pulse duration of 1.0 ns, the relative energy of the after-pulse decreases slightly with increasing pump power due to partial depletion of the gain by the primary pulse. However, after-pulsing still limits the useful energy to about 85% of the total output in this case. Because of the longer pulse duration of the secondary peak, generation of SBS is another important limitation, as illustrated in Fig 5b. Backwards-propagating SBS power can damage the seed laser and the isolators. Proper design of the microlaser should then target single-mode operation.

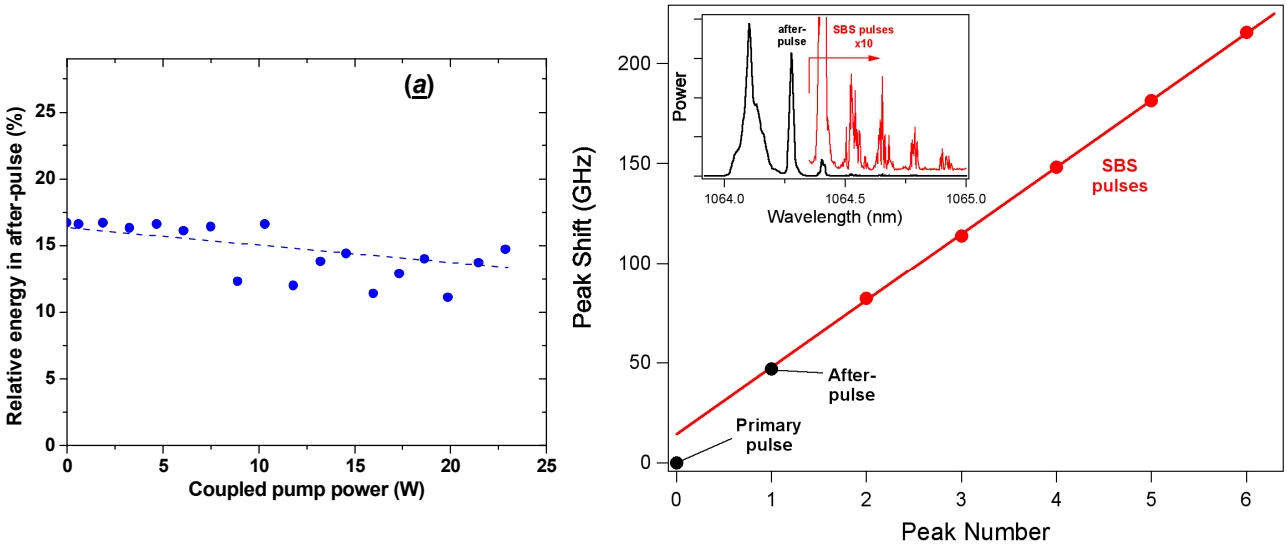

Fig. 5. (a) Variation of the secondary pulse energy with launched pump power; the LMA fiber amplifier and the seed microlaser are detailed in Ref. 11. (b) Observation of SBS generated by the after-pulse. The inset shows the spectrum of the amplifier output beam (co-propagating with the signal). The main graph shows the shift of each spectral peak shown in the inset with respect to the primary pulse. Linear extrapolation (red line) of the SBS peak positions (red circles) shows that SBS was generated by the after-pulse. The slope of the line (33.5 GHz) corresponds to two SBS shifts because each Stokes wave counter-propagates with respect to its pump beam; alternate Stokes orders (second, fourth, etc.) are thus present at the amplifier output.

3.5 Optimized high-energy amplifier

Commercial LMA fibers suitable for mode filtering are available with core diameters up to 30 μm, which have provided peak powers >1 MW and pulse energies >1 mJ.[2] At these power levels, effects associated with the nonlinear processes discussed in Section 2.1 were evident in the output temporal and spectral profiles. In order to investigate further power scaling, we characterized the performance of a LMA fiber with a larger core diameter (50 μm, 0.06 NA, 250 μm inner-cladding diameter, inner-cladding absorption 25 dB/m at 976 nm; Nufern). The fiber was polarization maintaining with a Panda design. The 1 m long fiber was loosely coiled with a diameter >10 cm and was seeded with the Yb^{3+}:YAG microlaser described in Section 3.3 to maximize the energy extraction.

Figure 6a shows the output energy as a function of pump power. The maximum pulse energy was 0.76 mJ at 1030.6 nm, corresponding to a peak power of 1.1 MW (Fig. 7). The spectrum was very clean, with no out-of-band power or ASE (Fig. 6b); the high-resolution spectrum showed modest broadening from SPM (Fig. 6b), with a linewidth of 0.17 nm FWHM. The polarization extinction ratio was >18 dB at 200 μJ and decreased to 9 dB at the maximum power.

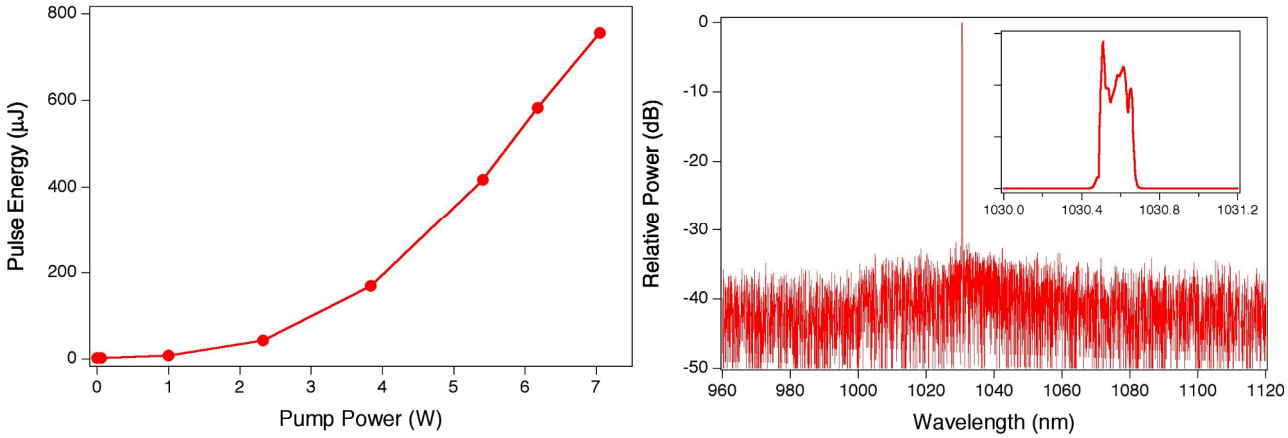

(a) (b)

Fig. 6. (a) Output pulse energy for the 50 μm core LMA fiber amplifier. Seed pulses were 4 μJ, 0.6 ns, at 1 kHz. (b) Semi-log scale output spectrum at 0.76 mJ. Inset: linear scale high resolution spectrum of amplified signal.

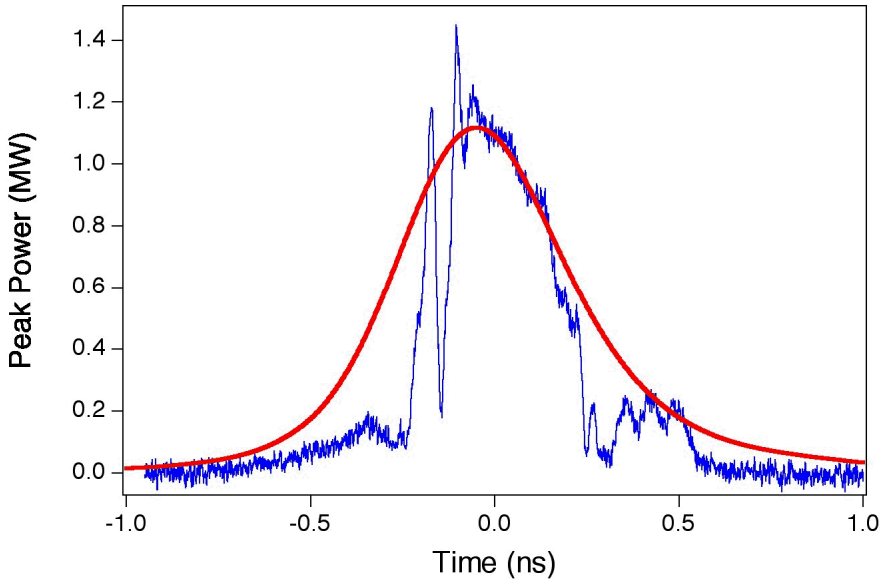

Fig. 7. Measured temporal profiles for two LMA fiber amplifiers with similar peak powers and at the same repetition rate (1 kHz). The red curve corresponds to the 50 μm fiber, and the blue curve to the 30 μm fiber of Ref. 2 (2 m long fiber seeded at 1064 nm with a pulse duration of 0.4 ns).

Figure 7 compares the temporal profile of the amplified pulse from the 50 μm fiber with that from a 30 μm LMA fiber with a similar peak power.[2] The drastic improvement in performance associated with the larger mode field area is evident. Similarly, spectral broadening due to SPM was much higher in the 30 μm fiber seeded with 0.67 ns pulses at 1064 nm: the measured linewidth was 0.3 nm at 250 μJ output energy,[11] 50% larger than the linewidth from the 50 μm fiber at more than 3x the output energy (760 μJ). The absence of an after-pulse further increases the useful power in the present system.

The output beam quality from the 50 μm fiber was variable and sensitive to handling of the fiber, indicating that coupling of the fundamental mode to high-order modes limits the performance of this fiber. Under some conditions, we achieved nearly diffraction-limited beam quality (M^2 = 1.25 and 1.29 in the two axes), but this performance could not be achieved routinely. Although generally more significant for larger core diameters, mode scrambling also depends strongly on properties of the fiber (e.g., refractive-index homogeneity) that are determined by the fiber fabrication and subsequent handling. The practical limit on core size will continue to increase as fiber manufacturing techniques advance. The present results with the 50 μm fiber and previous experiments with large-core fibers[26] suggest that the ultimate performance limit has not yet been reached with commercially available LMA fibers.

The high peak power (1.1 MW), smooth temporal profile, modest spectral broadening, and linear polarization state of the 50 μm fiber amplifier will allow very efficient nonlinear frequency conversion in a single-pass configuration.[11] These features are particularly interesting for pumping mid-IR optical parametric generators, with potential applications including remote chemical sensing and optical counter-measures. In that case, thermal lensing due to absorption of the idler beam limits power scaling and prohibits access to longer idler wavelengths; high pulse energy is critical because it provides high conversion efficiency without tight focusing, thereby alleviating the above limitations.[27] Pulsed fiber amplifiers thus extend the accessible range of power and wavelength compared to pumps with lower pulse energies and non-diffraction-limited beam quality.

Finally, we note that scaling the mode-field area of step-index LMA fibers is limited by bend-induced mode compression.[28-30] Based on current manufacturing capabilities and reasonable packaging constraints, the maximum mode field area for step-index fiber is ~600 μm^2, only 20% larger than that of the 30 μm LMA fiber. Novel approaches are being pursued to overcome this limitation, including more sophisticated refractive-index profiles[28,30] and operation on high-order modes.[8]

4. CONCLUSION

We reviewed some important design parameters for power scaling of pulsed fiber amplifiers. Due to the relative importance of the different nonlinear effects, a pulse duration close to 1.0 ns is optimum for minimizing spectral and temporal distortions of the amplified pulses. In this regime, the most limiting effect is FWM, amplified by SRS. Passively Q-switched microchip lasers offer numerous advantages for seeding of fiber amplifiers, enabling a simple and practical system architecture. Microchip-laser-seeded, mode-filtered fiber amplifiers have provided very high peak powers, pulse energies, and repetition rates with diffraction-limited beam quality and linear output polarization using a single-stage, single-pass amplifier with no high-speed or high-voltage electronics. For optimum performance of the fiber amplifier, the specifications of the microchip laser should be optimized, including wavelength and presence of an after-pulse. We showed that seeding the amplifier at 1030 nm rather than the more conventional wavelength of ~1060 nm can increase the pulse energy by 40%. With a LMA fiber with a 50 μm core diameter, we achieved up to 1.1 MW peak power and 0.76 mJ pulse energy with a smooth temporal profile, modest spectral broadening, and reasonable beam quality. Mode-filtered fiber amplifiers seeded by microchip lasers are an ideal pump sources for very efficient optical frequency conversion using standard nonlinear crystals in single-pass, non-resonant configurations.[11]

ACKNOWLEDGEMENT

Supported by Laboratory Directed Research and Development, Sandia National Laboratories, U.S. Department of Energy, under contract DE-AC04-94AL85000.

REFERENCES

[1] F. Di Teodoro and C. Brooks, "Multistage Yb-doped fiber amplifier generating megawatt peak-power, subnanosecond pulses," *Opt. Lett.* **30**, 3299-3301 (2005).

[2] R.L. Farrow, D.A.V. Kliner, P.E. Schrader, A.A. Hoops, S.W. Moore, G.R. Hadley and R.L. Schmitt, "High-peak-power (>1.2MW) pulsed fiber amplifier," in *Fiber Lasers III: Technology, Systems and Applications*, A. Brown, J. Nilsson, D. Harter and A. Tünnermann, eds. *Proc. SPIE* **6102**, 61020L-1/11 (2006).

[3] F. Di Teodoro and C. Brooks, "Multi-MW peak power single transverse mode operation of a 100 micron core diameter doped photonic crystal rod amplifier," *Fiber Lasers IV: Technology, Systems and Applications*, D. Harter, A. Tunnermann, J. Broeng and C. Headley eds. *Proc. SPIE* **6453**, 645318-1/5 (2007).

[4] J.P. Koplow, D.A.V. Kliner and L. Goldberg, "Single-mode operation of a coiled multimode fiber amplifier," *Opt. Lett.* **25**, 442-444 (2000).

[5] M. Ferman, "Single-mode excitation of multimode fibers with ultrashort pulses," *Opt. Lett.* **23**, 52-54 (1998)

[6] J. Limpert, A. Liem, M. Reich, T. Schreiber, S. Nolte, H. Zellmer, A. Tünnermann, J. Broeng, A. Petersson and C. Jakobsen, "Low-nonlinearity single-transverse-mode ytterbium-doped photonic crystal fiber amplifier," *Opt. Express* **12**, 1313-1319 (2004).

[7] H. Offerhaus, N. Broderick, D. Richardson, R. Sammuk, J. Caplen, L. Dong, "High-energy single-transverse-mode Q-switched fiber laser based on a multimode large-mode-area erbium-doped fiber," *Opt. Lett.* **23**, 1683-5 (1998).

[8] J.M. Fini and S. Ramachandran, "Natural bend-distortion immunity of higher-order-mode large-mode-area fibers," *Opt. Lett.* **32**, 748-750 (2007).

[9] J.-P. Fève, P.E. Schrader, R.L. Farrow and D.A.V. Kliner "Four-wave mixing in nanosecond pulsed fiber amplifiers," *Opt. Express* **15**, 4647-4662 (2007).

[10] J.-P. Fève, "Phase-matching and mitigation of four-wave mixing in fibers with positive gain," *Opt. Express* **15**, 577-582 (2007).

[11] P.E. Schrader, R.L. Farrow, D.A.V. Kliner, J.-P. Fève and N. Landru, "High power fiber amplifier with tunable repetition rate, fixed pulse duration, and multiple output wavelengths," *Opt. Express* **14**, 11528-11538 (2006).

[12] G. Agrawal, *Nonlinear Fiber Optics,* 3rd ed., Optics and Photonics Series (Academic, San Diego, Calif., 2001).

[13] P. Dragic, G. Papen and A. Galvanauskas, "Optical fiber with an acoustic guiding layer for stimulated Brillouin scattering suppression," in *Conference on Lasers and Electro-Optics*, paper CThZ3 (2005).

[14] M.J. Li, X. Chen, J. Wang, S. Gray, A. Liu, J. Demeritt, A. Ruffin, A. Crowley, D. Walton and L. Zenteno, "Al/Ge co-doped large mode area fibers with SBS threshold," *Opt. Express* **15**, 8290-8299 (2007).

[15] C. Brooks and F. Di Teodoro, "1-mJ energy, 1-MW peak power, 10-W average power, spectrally narrow, diffraction-limited pulses from a photonic-crystal fiber amplifier," *Opt. Express* **13**, 8999-9002 (2005).

[16] R.L. Farrow, D.A.V. Kliner, G.R. Hardley and A.V. Smith, "Peak-power limits on fiber amplifiers imposed by self-focusing," *Opt. Lett.* **31**, 3423-3425 (2006).

[17] A.V. Smith, B.T. Do and M. Soderlund, "Deterministic nanosecond laser-induced breakdown thresholds in pure and Yb^{3+} doped fused silica," *Fiber Lasers IV: Technology, Systems and Applications*, D. Harter, A. Tunnermann, J. Broeng and C. Headley eds. *Proc. SPIE* **6453**, 645317-1/12 (2007).

[18] S. Forget, F. Druon, F. Balembois, P. Georges, N. Landru, J.P. Feve, J. Lin, Z. Weng, "Passively Q-switched diode-pumped Cr^{4+}YAG/$Nd^{3+}GdVO_4$ microchip lasers," *Opt. Commun.* **259**, 816-819 (2006).

[19] R.L. Schmitt and B.T. Do, "Design and performance of a high-repetition-rate single-frequency Yb:YAG microlaser," *Solid State Lasers XVII: Technology and Devices*, *Proc. SPIE* **6871** (2008).

[20] J.-P. Feve, J. Morehead, S. Makki, J. Franke, M. Muendel, C. Wang and G. Zhao, "Q-switched fiber lasers with controlled pulse shape," *Fiber Lasers V: Technology, Systems and Applications*, *Proc. SPIE* **6871** (2008).

[21] J. Koponen, M. Söderlund, H.J. Hoffman. D.A.V. Kliner and J.P. Koplow, "Photodarkening measurements in large-mode-area fibers," *Fiber Lasers IV: Technology, Systems and Applications*, D. Harter, A. Tunnermann, J. Broeng and C. Headley eds. *Proc. SPIE* **6453**, 64531E-1/11 (2007).

[22] S. Jetschke, S. Unger, U. Ropke and J. Kirchhof, "Photodarkening in Yb doped fibers: experimental evidence of equilibrium states depending on the pump power," *Opt. Express* **15**, 14838-14843 (2007).

[23] J. Limpert, O. Schmidt, J. Rothhardt, F. Roser, T. Schreiber and A. Tunnermann, "Extended single-mode photonic crystal fiber lasers," *Opt. Express* **14**, 2715-2720 (2006).

[24] G. Spuhler, R. Paschotta, R. Fluck, B. Braun, M. Moser, G. Zhang, E. Gini and U. Keller, "Experimentally confirmed design guidelines for passively Q-switched microchip lasers using semiconductor saturable absorbers," *J. Opt. Soc. Am. B* **16**, 376-388 (1999).

[25] J.-P. Fève, N. Landru, and O. Pacaud, "Triggering Passively Q-switched Microlasers," in *Advanced Solid-State Photonics (TOPS)*, C. Denman and I. Sorokina, eds., Vol. 98 of OSA Trends in Optics and Photonics (Optical Society of America, 2005), paper 373.

[26] A. Galvanauskas, M.-Y. Cheng, K.-C. Hou, and K.-Hsiu Liao, "High peak power pulse amplification in large-core Yb-doped fiber amplifiers," *J. Sel. Top. Quantum Electron* **13**, 559-566 (2007).

[27] O. Pacaud, J.-P. Fève and L. Lefort, " Mid-Infrared Laser Source with High Average Power and High Repetition Rate," in *Conference on Lasers and Electro-Optics/Quantum Electronics and Laser Science and Photonic Applications, Systems and Technologies*, Technical Digest (CD) (Optical Society of America, 2005), paper PWA5.

[28] J.M. Fini, "Bend-compensated design of large-mode-area fibers," *Opt. Lett.*, **31**, 1963-1965 (2006).

[29] G.R. Hadley, R.L. Farrow and A.V. Smith, "Bent-waveguide modeling of large-mode-area, double-clad fibers for high-power lasers," *Fiber Lasers III: Technology, Systems, and Applications*, A.J.W. Brown, J. Nilsson, D.J. Harter, and A. Tünnermann eds., *Proc. SPIE* **6102**, 61021S-1/7 (2006).

[30] R.L. Farrow, G.R. Hadley, D.A.V. Kliner and J.P. Koplow, "Design of refractive-index and rare-earth-dopant distributions for large-mode-area fibers used in coiled high-power amplifiers," *Fiber Lasers IV: Technology, Systems and Applications*, D.J. Harter, A. Tünnermann, J. Broeng, and C. Headley eds., *Proc. SPIE* **6453**, 64531C-1/11 (2007).